

Tumour suppressor ING1b maintains genomic stability upon replication stress

Ronald P. C. Wong, Hanyang Lin, Shahram Khosravi, Brad Piche,
Seyed Mehdi Jafarnejad, David W. C. Chen and Gang Li*

Department of Dermatology and Skin Science, Jack Bell Research Centre, Vancouver Coastal Health Research Institute, University of British Columbia, Vancouver, British Columbia, ON, Canada V6H 3Z6

Received July 31, 2010; Revised December 16, 2010; Accepted December 20, 2010

ABSTRACT

The lesion bypass pathway, which is regulated by monoubiquitination of proliferating cell nuclear antigen (PCNA), is essential for resolving replication stalling due to DNA lesions. This process is important for preventing genomic instability and cancer development. Previously, it was shown that cells deficient in tumour suppressor p33ING1 (ING1b) are hypersensitive to DNA damaging agents via unknown mechanism. In this study, we demonstrated a novel tumour suppressive function of ING1b in preserving genomic stability upon replication stress through regulating PCNA monoubiquitination. We found that ING1b knock-down cells are more sensitive to UV due to defects in recovering from UV-induced replication blockage, leading to enhanced genomic instability. We revealed that ING1b is required for the E3 ligase Rad18-mediated PCNA monoubiquitination in lesion bypass. Interestingly, ING1b-mediated PCNA monoubiquitination is associated with the regulation of histone H4 acetylation. Results indicate that chromatin remodelling contributes to the stabilization of stalled replication fork and to the regulation of PCNA monoubiquitination during lesion bypass.

INTRODUCTION

Unrepaired DNA lesions, such as photolesions generated by UV radiation, stall replication forks progression because replicative DNA polymerases are unable to recognize modified DNA bases (1). Stalled replication may have serious consequences such as replication collapse, DNA double-strand breaks (DSBs), recombination and genomic instability (2). Stalled replication caused by UV lesions can be circumvented by the replication bypass mechanisms including the error-prone translesion DNA synthesis (TLS) (3), or the error-free template switching

pathway (4) which are regulated by monoubiquitination or polyubiquitination of proliferating cell nuclear antigen (PCNA), respectively (5,6). Both pathways require initial modification of PCNA by monoubiquitination at the Lys164 residue by the E2 ubiquitin-conjugating enzyme Rad6 and the E3 ligase Rad18 upon replication stress (7–10). Monoubiquitinated PCNA (PCNA-Ub) alters affinity of Y-family polymerases PCNA to the ubiquitin-binding domain of PCNA. These polymerases are functional even when DNA lesions are present since they can accommodate the lesions at their active sites, replicating across the lesion (11). Pol η is a member of the Y-family polymerases which is able to replicate across UV lesions (12,13). Pol η is recruited to the sites of replication and colocalizes with PCNA and Rad18 in foci upon UV irradiation (8,9,14). Cells derived from patients with xeroderma pigmentosum variant (XPV) which are deficient in Pol η exhibit a prolonged S phase arrest and enhanced H2AX phosphorylation following UV exposure, suggesting that the DSBs may arise from replication fork collapse (15,16). There is a higher incidence for sunlight-induced skin cancers in XPV patients (17) suggesting the importance of resolving stalled replication during cancer development. However, the regulation of PCNA-Ub-mediated recovery of stalled replication is not well understood.

The inhibitor of growth (ING) proteins regulate various biological processes including cell cycle progression, apoptosis, DNA repair and senescence. They are frequently found to be inactivated in cancers. ING proteins contain a structurally conserved PHD domain at the C terminus that binds to histone H3 trimethylated at lysine 4 (18,19). ING proteins are components of various histone acetyltransferase (HAT) and histone deacetylase (HDAC) complexes. Therefore, they partly carry out their functions through chromatin remodelling (20–23). Recently, it has been shown that ING2 is required for normal DNA replication (24), and ING5 is found in a complex with the HBO1 HAT which is also required for DNA replication (20). However, the role of ING proteins in replication stress is not known. Previously, we and others have showed that ING1b knockdown (KD)

*To whom correspondence should be addressed. Tel: +1 604 875 5826; Fax: +1 604 875 4497; Email: gangli@interchange.ubc.ca

sensitized S phase arrested melanoma cells to UV (25) and MEFs from knockout mice exhibited increased sensitivity to UV (26). However, the mechanism for UV hypersensitivity in ING1-deficient cells is unclear. In this study, we found that depletion of physiological level of ING1b sensitizes cells to UV. ING1b KD cells exhibit defects in recovering from UV-induced stalled replication and enhanced genomic instability. We further found that ING1b plays a role in the lesion bypass pathway. Moreover, ING1b is required for the E3 ligase Rad18-mediated PCNA-Ub and for Rad18 and Pol η to be tethered to the chromatin at the sites of replication. Interestingly, ING1b KD cells showed hypoacetylation at S phase and restoration of histone acetylation in ING1b KD cells rescued PCNA-Ub and Rad18 binding to chromatin. These data suggest a novel tumour suppressor function of ING1b in regulating the lesion bypass pathway through PCNA monoubiquitination and chromatin remodelling to preserve genomic stability upon replication stress.

MATERIALS AND METHODS

Cell culture, antibodies, expression plasmids, chemicals and UV irradiation

HCT116 and HEK293 cells were cultured in Dulbecco's Modified Eagle Media (DMEM) (Invitrogen, Burlington, ON, Canada) supplemented with 10% fetal bovine serum (Invitrogen), 100 U/ml penicillin and 100 μ g/ml streptomycin (Invitrogen) in 5% CO₂ humidified atmosphere at 37°C. Anti-actin and rabbit anti-Flag antibodies were purchased from Sigma-Aldrich (St Louis, MO, USA); anti-BrdU from BD Biosciences; anti- γ H2AX (Ser 139) and anti-PCNA from Millipore (Billerica, MA, USA); anti-AcH4K5/8/12/16, anti-AcH3K9/14 and anti-H4 from Millipore; anti-ubiquitin, BRG1, ING1b, Lamin B1 and pATM (Ser 1981) from Santa Cruz Biotechnology (Santa Cruz, CA, USA); anti-Rad18 from Abnova (Walnut, CA, USA); anti-SNF5 from Abcam (Cambridge, MA, USA); anti-CPD from Cosmo Bio (Tokyo, Japan); and mouse anti-Flag from Applied Biological Materials (Richmond, BC, Canada). BrdU was purchased from Sigma-Aldrich. UV irradiation was performed by removal of medium, washing with PBS and exposure to controlled dose of UVC (254 nm) light using a cross-linker (UltraLum, Claremont, CA, USA). Flag-Pol η is a gift from Dr A.R. Lehmann and p3xFlag14-HsRad18 is a gift from Dr K. Myung.

Expression plasmid, siRNA transfections and shRNA construction

Expression plasmids were transfected into HCT116 cells by Effectene Transfection Reagent (Qiagen, Mississauga, ON, Canada) according to the manufacturer's instruction. UV irradiation and assays were performed at 24 h after transfection. siRNAs were synthesized by Qiagen. Two ING1b siRNAs were used with target sequences as follows: siRNA-1: 5'-accacgtactgtctgtgcaa-3' and siRNA-2: 5'-ttggtacacgtgtaacaagaa-3', and the target sequence for Rad18 siRNA is 5'-atggtgtgcccaggttaa-3'.

siRNA was transfected to cells by siLenFect Lipid reagent (Bio-Rad, Mississauga, ON, Canada) according to manufacturer's instruction. Assays were performed 48 h after transfection.

Short-hairpin RNA targeting ING1b sequence 5'-aacatgttgagtctgctgcaa-3' was constructed using HuSH-29 shRNA system (Origene, Rockville, MD, USA) according to the manufacturer's instruction. In brief, shRNA cassette was generated by annealing top and bottom strands of the oligos containing shRNA target sequence and was cloned into BamHI and HindIII cloning sites on the pRS vector with U6 promoter. pRS vector and ING1b-shRNA were transfected into the retroviral packaging cell line, Phoenix Amphi cells (Orbigen, San Diego, CA, USA). Retroviral particles were collected 3 days after transfection and concentrated by ultracentrifugation. pRS vector and ING1b shRNA retroviral particles were used to infect HEK293. Infected cells were selected with 1 μ g/ml puromycin. Stable KD was confirmed by western blot.

Subcellular fractionation

Fractionation of chromatin bound and unbound fractions were described previously (9,25). Briefly, cytoplasmic and nucleoplasmic proteins were isolated by cytoskeletal buffer (CSK) (100 mM NaCl, 300 mM sucrose, 3 mM MgCl₂, 10 mM PIPES pH 6.8, 1 mM EGTA, 0.2% Triton X-100) with protease inhibitors for 15 min on ice. After centrifugation at 900g for 5 min at 4°C, chromatin bound proteins in the pellet were resuspended in modified RIPA buffer (150 mM NaCl, 50 mM Tris-HCl, pH 7.4, 1 mM EDTA, 0.1% NP-40, 0.25% sodium dodecyl sulphate) and sonicated.

Histone extraction, western blot and immunoprecipitation

Cells were lysed in cell lysis buffer (10 mM Tris-HCl, pH 7.5, 1 mM MgCl₂ and 0.5% NP-40) for 10 min on ice. Nuclei were pelleted by centrifugation at 1000g for 5 min at 4°C. Nuclei were resuspended in extraction buffer (0.5 M HCl, 10% glycerol and 0.1 M β -mercaptoethanol) for 1 h on ice. After centrifugation at 10000g, the acid-soluble fraction was taken and neutralized by 2 M NaOH. Proteins were quantified and prepared for western blotting as described (25) using the Odyssey Infrared Imaging System (LI-COR, Lincoln, NE, USA) equipped with Odyssey 2.1 software.

For immunoprecipitation, cells were resuspended in modified RIPA buffer followed by incubation with 2 μ g of specific antibody at 4°C overnight. Immunocomplex was pulled down by 50 μ l protein G, washed thrice with modified RIPA for 5 min followed by WB. For immunoprecipitation of Pol η , cells were incubated with 1% formaldehyde 10 min at room temperature for cross-linking followed by stopping the reaction with 0.125 M glycine prior to lysis with cell lysis buffer. The nuclei were resuspended in modified RIPA followed by immunoprecipitation with specific antibody.

Immunofluorescence

Cells were fixed with 1% paraformaldehyde in $1 \times$ PBS for 10 min at room temperature and permeabilized with methanol/acetone (1:1) at -20°C for 10 min. For BrdU staining, the slides were treated with 2N HCl for 10 min at room temperature followed by neutralization with sodium borate (pH 10.5) for 5 min. The slides were incubated with specific primary antibodies followed by incubation with Alexa Fluor 488 anti-mouse and Alexa Fluor 568 anti-rabbit secondary antibodies (Invitrogen, CA, USA). The slides were mounted with Vectorshield mounting media with DAPI (Vector Laboratories, CA, USA). The images were obtained by a laser scanning confocal microscope, LSM 780, equipped with the ZEN software, under the $10\times$ eyepiece and $63\times$ oil immersion lens (Carl Zeiss, ON, Canada). Ten to fifteen optical sections each with $0.4\mu\text{m}$ distance in the z -direction were obtained for each image. The images were further processed into 2D by maximum intensity projection provided from the ZEN software. The weighted colocalization coefficient of BrdU staining with Rad18 staining was calculated using the colocalization module equipped in the ZEN software under the same threshold values for all images. The number of Rad18 foci was quantified with the Image J software.

Analysis of metaphase chromosome

Cells were arrested at G1 by serum starvation, irradiated with or without UV and released in the presence of $0.1\mu\text{g/ml}$ colcemid for 18 h. Cells were trypsinized and resuspended with 0.5ml of medium. Ten millilitre of 0.075M KCl was added slowly and gently. Cells were incubated at 37°C for 15 min. Three to five drops of fixative (3:1 methanol/acetic acid) were added to stop the reaction and the cells were centrifuged at 1200 for 8 min. Supernatant was removed, leaving 0.5ml to resuspend the pellet. Ten millilitre of fixative was added gently and slowly. Cells were pelleted, resuspended and fixed in the same way twice. The pellet was finally resuspended in 0.5ml of fresh fixative. Chromosome preparation ($30\mu\text{l}$) was dropped on a pre-chilled microslide and let spread by gravity. Chromosomes were stained with a 1:20 Giemsa stain (Sigma-Aldrich) for 20 min, washed with water and mounted with Cytoseal 60 mounting medium (Fisher Scientific, Ottawa, ON, Canada). The slides were observed under a microscope (Zeiss, Toronto, ON, Canada) with a $100\times$ oil immersion lens and $10\times$ eyepiece. An image was obtained using a QImaging Ketiga Ex camera and was analysed with Northern Eclipse software.

Replication fork progression by qPCR

Cells were trypsinized and resuspended in lysis buffer (5mM Tris-HCl, 100mM EDTA pH 8.0, 1% SDS and $80\mu\text{g/ml}$ proteinase K) and incubated at 55°C for 2 h. Genomic DNA was isolated by phenol/chloroform extraction. Genomic DNA (250ng) was used for qPCR analysis of DNA replication using SYBR PCR Master Mix with the 7900 HT Fast Real-time PCR system

(Applied Biosystems, Carlsbad, CA, USA). Primers used were as follows: Ori, $5'$ -ccagaatccgatgcacc- $3'$ (forward), $5'$ -tccgttttgcaggtgtgc- $3'$ (reverse); 3.5 kb distal to the Ori, $5'$ -ctgggtgcagatccagtt- $3'$ (forward), $5'$ -atggteccaggatacaca- $3'$ (reverse); and β -globin, $5'$ -caacttcacccagttcacc- $3'$ (forward), $5'$ -acacaactgtgtcac tagc- $3'$ (reverse). qPCR conditions: dissociation, 95°C , 30 s; and annealing/extension, 60°C , 1 min.

Cell synchronization

For synchronization at G1, cells were starved in serum free medium for 24 h. For cell synchronization at the G1-S boundary, cells were treated with 2mM thymidine for 17 h and released into fresh medium for 8 h followed by a second thymidine block or treatment with $1\mu\text{g/ml}$ aphidicolin for 14 h.

Sulphorhodamine B assay

Cells were fixed in 10% trichloroacetic acid for 1 h at 4°C , rinsed and dry, followed by staining with 0.057% sulphorhodamine B for 15 min at room temperature (27). Stained plates were washed with 1% acetic acid thrice and let dry. SRB dye from the stained cells was dissolved in 10mM Tris-HCl (pH 10.5). Absorbance at 550nm was measured.

RESULTS

ING1b KD cells are more sensitive to UV at S phase

We investigated the physiological role of ING1b in UV response in HCT116 cells, which retain normal DNA damage checkpoint (28,29). This cell line expresses wild-type ING1b (data not shown) and p53 which is required for many functions of ING proteins (30,31). We knocked down ING1b expression with 70% KD efficiency at 48 h after siRNA transfection (Figure 1A). We found that ING1b KD sensitized cells to UV (Figure 1B). We generated stable ING1b KD cells by shRNA in HEK293 cells and found that ING1b shRNA cells were more sensitive to UV (Supplementary Figure S1), which is consistent with the hypersensitivity of ING1b-deficient cells to UV (25,26). Since we showed previously that ING1b is required for NER (25), we analysed the persistence of UV-induced DNA lesions in control and ING1b KD HCT116 cells (Supplementary Figure S2). Consistent with our previous finding (25), repair of UV lesions is retarded in ING1b KD cells. However, we found that the extent of DNA lesions was comparable in control and ING1b KD cells up to 12 h after UV, suggesting that the sensitization of ING1b KD cells to UV at this time is probably not due to the difference in NER efficiency in these cells. We further analysed the effect of ING1b KD on progression of cells from G1 to G2/M in a single cell cycle. Without UVR, ING1b KD cells progressed from G1 to G2/M $\sim 4\text{h}$ faster than the control cells (Figure 1C and Supplementary Figure S3). This is consistent with the role of ING1b in cell proliferation (32,33). On the other hand, we observed that there was a significant increase in the sub-G1 cell

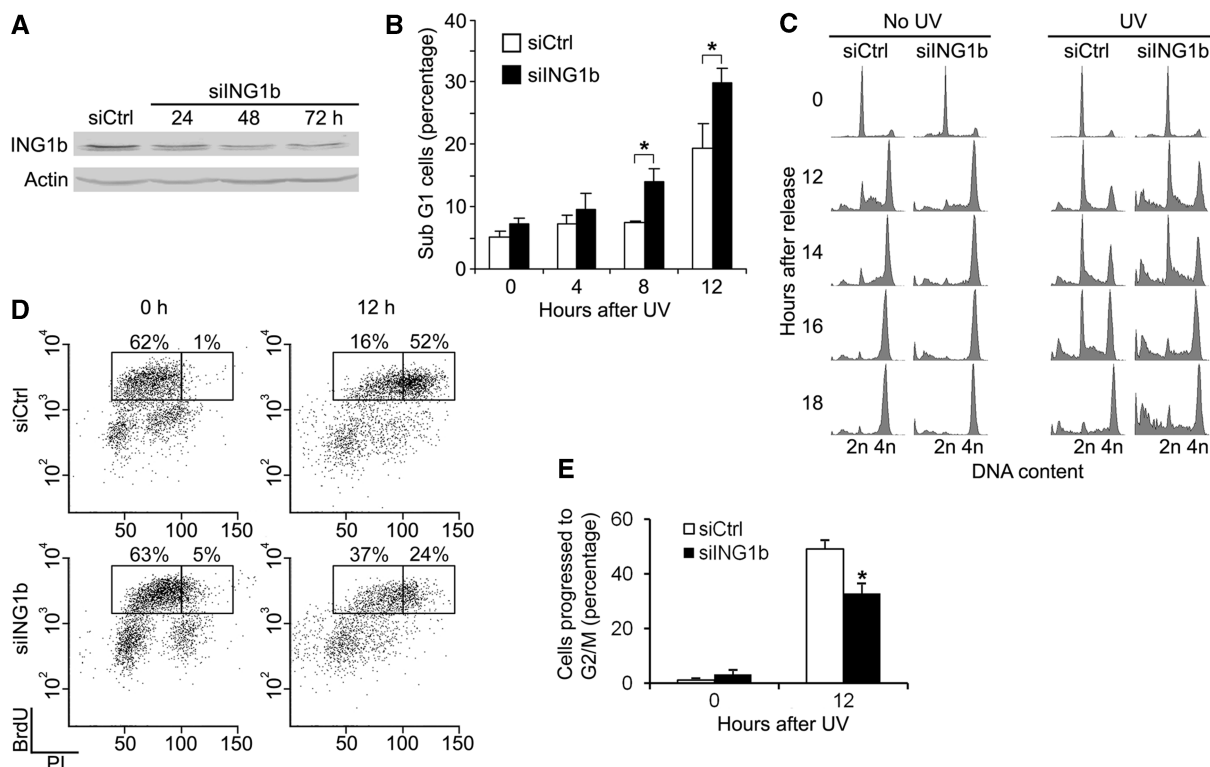


Figure 1. ING1b KD sensitizes cells to UV at S phase. (A) HCT116 cells were transfected with control or ING1b siRNA and harvested for western blot (WB) at various time points. (B) ING1b KD sensitizes cells to UV. HCT116 cells were transfected with control or ING1b siRNA, irradiated with 10J/m^2 UVC, and harvested at indicated times after UV for PI staining followed by FACS analysis. Data was shown as mean \pm SEM from three independent experiments ($^*P < 0.05$). (C) Cell cycle analysis for ING1b KD cells. Control or ING1b KD HCT116 cells were arrested at G1 by serum starvation, irradiated with 10J/m^2 UVC and released in the presence of 50 ng/ml nocodazole followed by cell cycle analysis. (D) ING1b KD cells fail to recover from stalled replication. Control or ING1b KD HCT116 cells were pulsed with $20\mu\text{M}$ BrdU, irradiated with 10J/m^2 UVC and chased for 12 h. Cells were stained with anti-BrdU antibody and PI, and analysed by FACS. (E) Quantification of BrdU-labelled cells in G2/M phase from three independent experiments ($^*P < 0.05$).

population in ING1b KD cells after UVR indicating that more cells were undergoing cell death (Figure 1C and Supplementary Figure S3). We observed a significant increase in cells accumulated at S phase in ING1b KD cells 12 and 14 h after UV (Figure 1C and Supplementary Figure S3C); therefore, we examined if increased cell death in ING1b KD cells after UV irradiation is due to the inability of these cells to complete S phase. We pulsed the cells with BrdU to label cells undergoing DNA replication and quantified the percentage of cells progressed to G2/M 12 h after UV. We found that the percentage of BrdU labelled cells that had progressed to G2/M was significantly reduced in ING1b KD cells compared with control (Figure 1D and E). Meanwhile, ING1b KD did not affect S phase progression in non-irradiated cells (Supplementary Figure S4). These data indicate that ING1b KD cells contain defects in S phase recovery after UV but not in non-stress conditions. We further pulsed the cells with BrdU at different time points after UV and observed that ING1b KD reduced BrdU incorporation in S phase as indicated by a ‘flattened’ pattern in the BrdU positive population indicating that more extensive stalled replication occurred in the ING1b KD cells (Supplementary Figure S5). These results suggest that cells lacking ING1b expression are

defective in recovering from UV-induced stalled replication and thus fail to progress to G2/M, becoming apoptotic.

ING1b KD cells show defects in replication fork progression and enhanced genomic instability after UV

To further demonstrate the importance of ING1b for replication fork progression after UV, we analysed the amplification of genomic DNA at a known replication origin in the *lamin B2* gene (34) by qPCR. We isolated genomic DNA from cells released from the G1–S boundary and analysed DNA replication at the origin (Ori) and a region 3.5 kb distal to the origin at different time points after UV (Figure 2A). The amount of replicated DNA was significantly reduced in ING1b KD cells compared with control cells at 60 min (compare 1 versus 2 and 3 versus 4, Figure 2B). This was even more prominent at 240 min after UV (compare 5 versus 6 and 7 versus 8, Figure 2B), indicating that the ability of the replication fork to progress from the origin to 3.5 kb distal is impaired in cells lacking ING1b expression after UV. The effect of ING1b KD is less prominent during non-stress conditions (Supplementary Figure S6).

We speculated that ING1b prevents the stalled replication forks from collapsing. It is believed that UV-induced

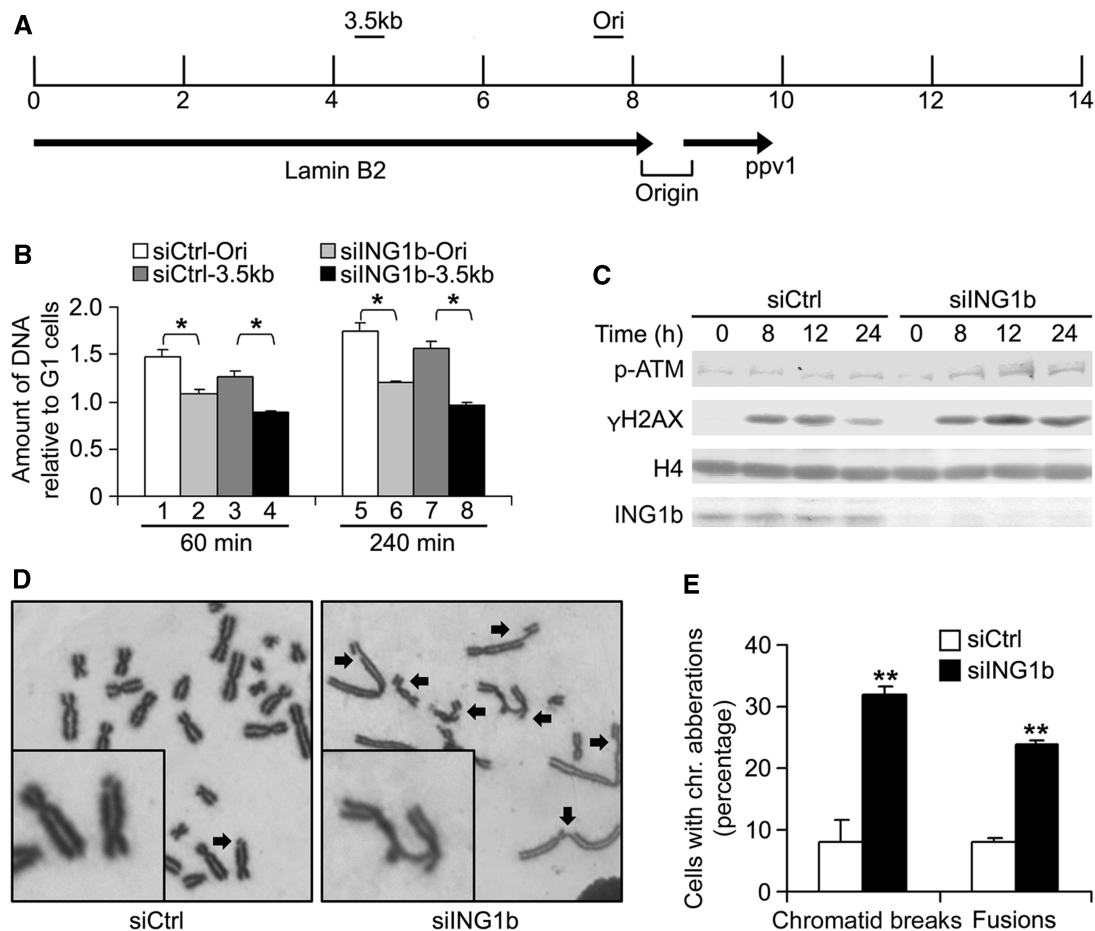


Figure 2. ING1b KD cells show defects in replication fork progress and enhanced genomic instability after UV. (A) Schematic diagram for the replication origin at *lamin B2* gene. Primers designed for the origin (Ori) and 3.5 kb distal of the origin (3.5 kb) are indicated. (B) Stalled replication at *lamin B2* replication origin in ING1b KD cells after UV. Control and ING1b KD HCT116 cells were arrested at G1-S boundary, irradiated with 10J/m^2 UVC and released for 60 and 240 min. Genomic DNA was isolated and analysed by qPCR. All samples were normalized with β -globin gene, a region replicated at late S phase. Relative replicated DNA was calculated by amount of DNA in cells after release over amount of DNA in G1 arrested cells. Data was presented as mean \pm SEM from three independent experiments ($*P < 0.05$). (C) Enhanced and prolonged γ H2AX and pATM after UV. Control and ING1b KD HCT116 cells were irradiated with 10J/m^2 UVC, WCE and histones are extracted for WB. (D) Representative images of metaphase chromosome. Control and ING1b KD HCT116 cells were arrested at G1 by serum starvation, irradiated with 10J/m^2 UVC and released in the presence of $0.1\mu\text{g/ml}$ colcemid for 18 h. Metaphase chromosome was prepared on slides and stained with Giemsa stain. Arrow indicates chromosome aberrations. (E) Quantification of chromosomal aberrations. Percentage of cells containing chromatid breaks or chromosome fusions was counted. Thirty cells were counted on each slide and the experiment was done in triplicate ($**P < 0.01$).

DSBs are caused by collapse of replication forks arrested at the UV lesions (15). Therefore, we analysed the levels of H2AX phosphorylation at Ser139 (γ H2AX) and phosphorylation of ATM at Ser 1981 which occur upon DSBs. We detected an increased level of γ H2AX and pATM in ING1b KD cells when compared with control (Figure 2C), indicating that DSBs are more extensive in ING1b KD cells after UV. We further observed an increased number of aberrant structures in metaphase chromosomes in ING1b KD cells, a 4-fold increase in chromatid breaks and a 3-fold increase in chromosomal fusions, which appear to be chromatid exchange, compared with control cells after UV (Figure 2D and E). We observe a very low level of spontaneous chromosome aberrations in control and ING1b KD cells (Supplementary Figure S7). Together, these data suggest that ING1b plays an important role in the response to

UV-induced replication stress, preserving the genomic stability.

ING1b regulates PCNA monoubiquitination and TLS

We sought to elucidate the mechanism by which ING1b regulates replication fork stability upon during replication stress. As PCNA-Ub is essential for the lesion bypass pathway with respect to overcoming replication blockage, we investigated if ING1b regulates PCNA-Ub. We detected the monoubiquitinated form of PCNA by western blotting which was induced by UV (Supplementary Figure S8). ING1b KD decreased PCNA-Ub by 40 and 70% at 6 and 24 h after UV, respectively, in HCT116 cells (Figure 3A), which indicates that PCNA-Ub is inhibited rather than delayed in ING1b KD cells. We also observed a reduction of PCNA-Ub in

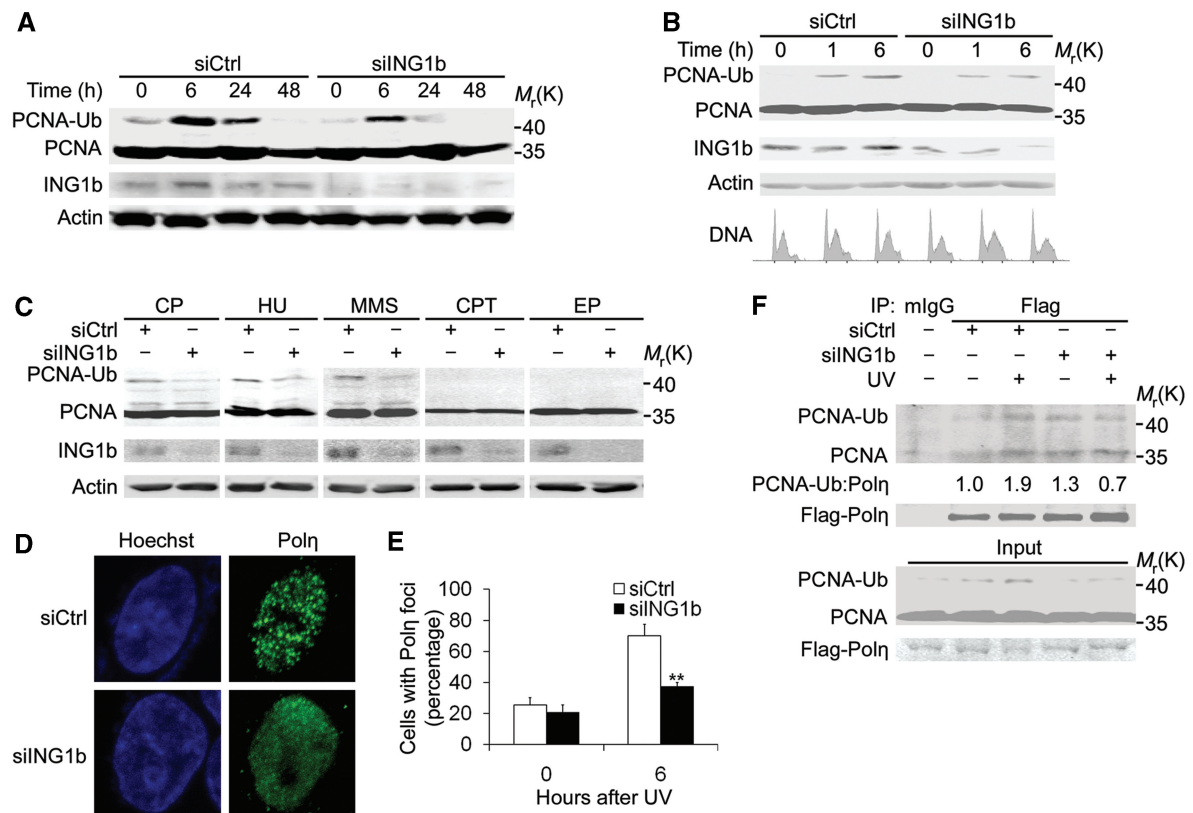


Figure 3. ING1b regulates PCNA-Ub and Pol η foci formation upon replication stress at S phase. (A) ING1b KD reduces PCNA-Ub after UV. Control and ING1b KD HCT116 cells were irradiated with 10 J/m² UVC for indicated times. Chromatin fraction was isolated for WB. (B) ING1b is required for efficient PCNA-Ub at S phase. Control and ING1b KD HCT116 cells were synchronized at G1-S boundary as in Figure 2B, released for 3 h into S phase and irradiated with 10 J/m² UVC. Chromatin fraction was isolated for WB. DNA content was analysed by FACS. (C) ING1b is required for PCNA-Ub upon replication stress. Control and ING1b KD HCT116 cells were treated with 100 μ M CP for 1 h and replaced with fresh media for 5 h, 10 mM HU for 6 h; and 250 μ M MMS, 0.25 μ M CPT or 20 μ M EP for 4 h. Chromatin fraction was isolated for WB. (D) ING1b is required for Pol η foci formation after UV. HCT116 cells transfected with Flag-tagged Pol η were irradiated with 10 J/m² UVC for 6 h. Cells were fixed and observed under confocal fluorescence microscope. (E) Quantification of number of cells displaying Pol η foci. Fifty cells were counted on each slide and the experiment was done in triplicate (** $P < 0.01$). (F) Pol η interaction with PCNA-Ub is reduced in ING1b KD cells. Control and ING1b KD HCT116 cells transfected with Flag-Pol η were irradiated with 10 J/m² UVC for 6 h. IP for nuclear Flag-Pol η were performed as described in Supplementary Experimental Methods. Relative interaction of Pol η with PCNA-Ub was calculated by quantifying the band intensity of PCNA-Ub over that of Pol η in the IP fraction (PCNA-Ub:Pol η).

normal human fibroblasts and HEK293 cells upon ING1b depletion (Supplementary Figure S9A and B). To confirm that inhibition of PCNA-Ub by ING1b KD was not due to the off-target effect, we treated cells with another ING1b siRNA and found that it also reduced PCNA-Ub after UV (Supplementary Figure S9C). Furthermore, inhibition of PCNA-Ub was also observed when cells were irradiated with a much lower dose of UV (1 J/m²) (Supplementary Figure S10). Since PCNA-Ub occurs predominantly at S phase (35), we asked if ING1b affects PCNA-Ub at S phase. We synchronized cells at G1-S boundary and released them into S phase (Figure 3B, bottom panel) followed by UV irradiation. We observed a reduction of PCNA-Ub in ING1b KD cells after UV compared with the control (Figure 3B). PCNA-Ub is induced by various genotoxic agents, such as cisplatin, hydroxyurea and methyl methanesulphonate, all of which stall replication forks and lead to appearance of ssDNA (5,6,9). We then treated control and ING1b KD cells with these agents and found that ING1b KD inhibited PCNA-Ub induced by these agents, while PCNA-Ub was

not detected in cells treated with etoposide and camptothecin which induce DSBs rather than stalling of replication (Figure 3C). It was shown previously that translesion DNA polymerase Pol η preferentially interacts with the monoubiquitinated form of PCNA (9). We asked if ING1b is required for Pol η foci formation after UV. We found that Pol η foci formation significantly increased after UVR but was dramatically reduced in ING1b KD cells (Figure 3D and E). In addition, Pol η interaction with monoubiquitinated PCNA (Figure 3F) and Pol η binding to chromatin (Supplementary Figure S11) after UV were reduced in ING1b KD cells. Our data suggest that ING1b regulates PCNA-Ub in S phase during replication fork stalling and facilitates Pol η -dependent lesion bypass to avoid catastrophic consequence from replication fork collapse.

ING1b is required for Rad18-mediated PCNA-Ub

We further examined if ING1b is required for PCNA-Ub mediated by the Rad18 E3 ligase. Ectopic expression of Rad18 enhanced PCNA-Ub in control cells in a

time-dependent manner after UV. Rad18-enhanced PCNA-Ub was abrogated in ING1b KD cells at 1 h and more dramatically at 6 h (Figure 4A). Moreover, we observed a corresponding reduction of Rad18 binding to chromatin in ING1b KD cells when compared with the control while the total Rad18 expression did not change significantly (Figure 4A). We then knocked down the expression of ING1b and Rad18 alone or in combination, and found that co-KD of ING1b and Rad18 resulted in a further reduction in PCNA-Ub and sensitized cells to UV compared to ING1b and Rad18 KD alone (Supplementary Figure S12). We further asked how ING1b regulates Rad18 functions. Rad18 is known to colocalize with sites of replication (8). We labelled sites of replication by pulsing cells with BrdU prior to UV and performed immunofluorescent staining for Rad18 and BrdU. We found that Rad18 formed punctate foci which colocalized with BrdU in control cells after UV (Figure 4B–D). Rad18 foci formation was abrogated in ING1b KD cells while BrdU foci could still be observed in these cells (Figure 4B–D). Furthermore, UV induced interaction between Rad18 with PCNA in control cells while this association was dramatically reduced in ING1b KD cells (Figure 4E). These data suggest that ING1b is required for the engagement of Rad18 on

chromatin at the sites of replication during replication blockage to mediate PCNA-Ub.

ING1b maintains histone H4 acetylation during S phase and is required for Rad18-mediated PCNA-Ub

We further studied the mechanism by which ING1b regulates PCNA-Ub. We previously showed that ING1b is required for histone H4 acetylation (AcH4) during the repair of UV-damaged DNA (25). We asked whether ING1b affects histone H3 and H4 acetylation at S phase. We synchronized cells at the G1-S boundary, released them into S phase and irradiated the cells with UV. We then examined the acetylation level of H3 and H4 and found that both AcH3 and AcH4 levels increased moderately after UV in control cells. We observed a dramatic decrease in AcH4 level in ING1b KD cells when compared to control cells whereas only a slight reduction was seen for AcH3 (Figure 5A and Supplementary Figure S10). We postulated that ING1b-regulated AcH4 might be important in PCNA-Ub. We first studied the effect of histone hyperacetylation induced by trichostatin A (TSA), a histone deacetylase (HDAC) inhibitor. TSA treatment enhanced AcH4 and PCNA-Ub after UV (Figure 5B). Furthermore, TSA treatment at various doses restored AcH4 and PCNA-Ub

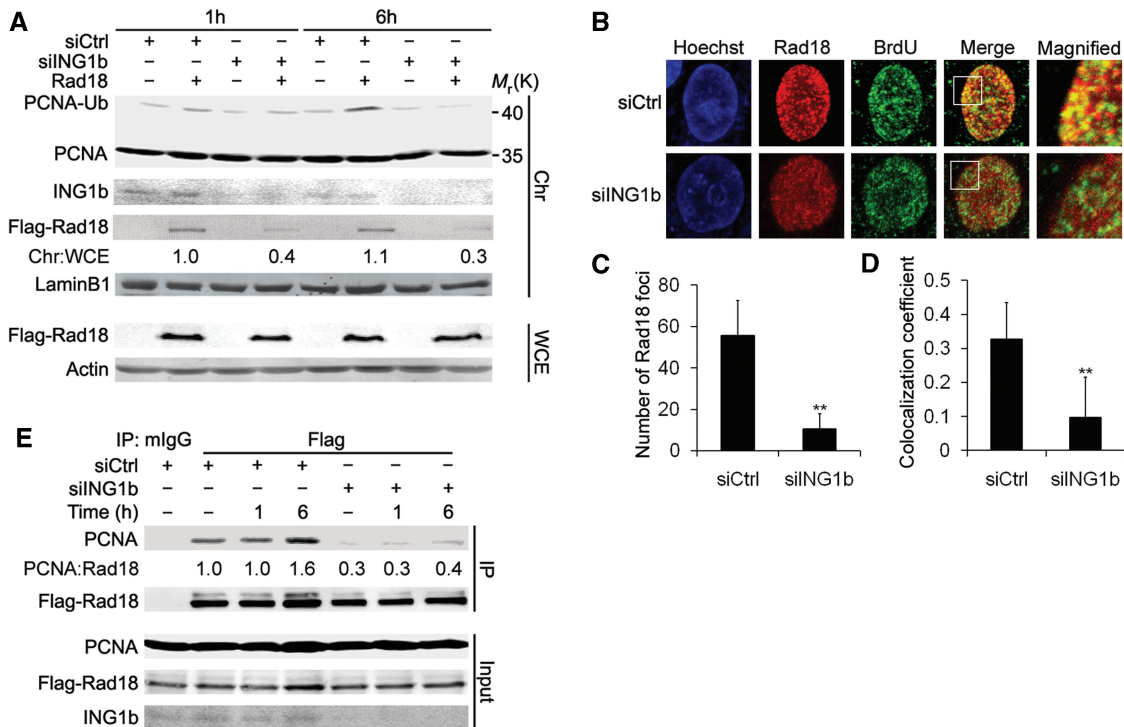


Figure 4. ING1b is required for Rad18-mediated PCNA-Ub during stalled replication. (A) ING1b is required for Rad18-mediated PCNA-Ub. Control and ING1b KD HCT116 cells were transfected with either vector control or Flag-Rad18 plasmid. Cells were irradiated with $10\text{J}/\text{m}^2$ UVC and whole cell extract (WCE) or chromatin bound proteins (Chr) were analysed by WB. Relative binding of Rad18 to chromatin is calculated as Chr:WCE. (B) ING1b is required for Rad18 foci formation at S phase after UV. Control and ING1b KD HCT116 cells were transfected with Flag-Rad18 plasmid. Cells were pulsed with $20\mu\text{M}$ BrdU and irradiated with $10\text{J}/\text{m}^2$ UVC for 1 h. Immunofluorescent staining was performed using anti-BrdU and Flag antibodies. White box indicates the portion of nucleus displayed on the magnified panel. (C) Number of Rad18 foci was quantified by Image J. (D) Weighted colocalization coefficient of BrdU staining with Rad18 staining was analysed with ZEN software. Thirty cells were counted on each slide and the experiments were done in triplicate (** $P < 0.01$). (E) ING1b is required for Rad18-PCNA interaction. Control and ING1b KD HCT116 cells were transfected with Flag-Rad18, irradiated with or without $10\text{J}/\text{m}^2$ UVC. Immunoprecipitation was performed using anti-Flag antibody. Relative Rad18-PCNA interaction is calculated as PCNA:Rad18.

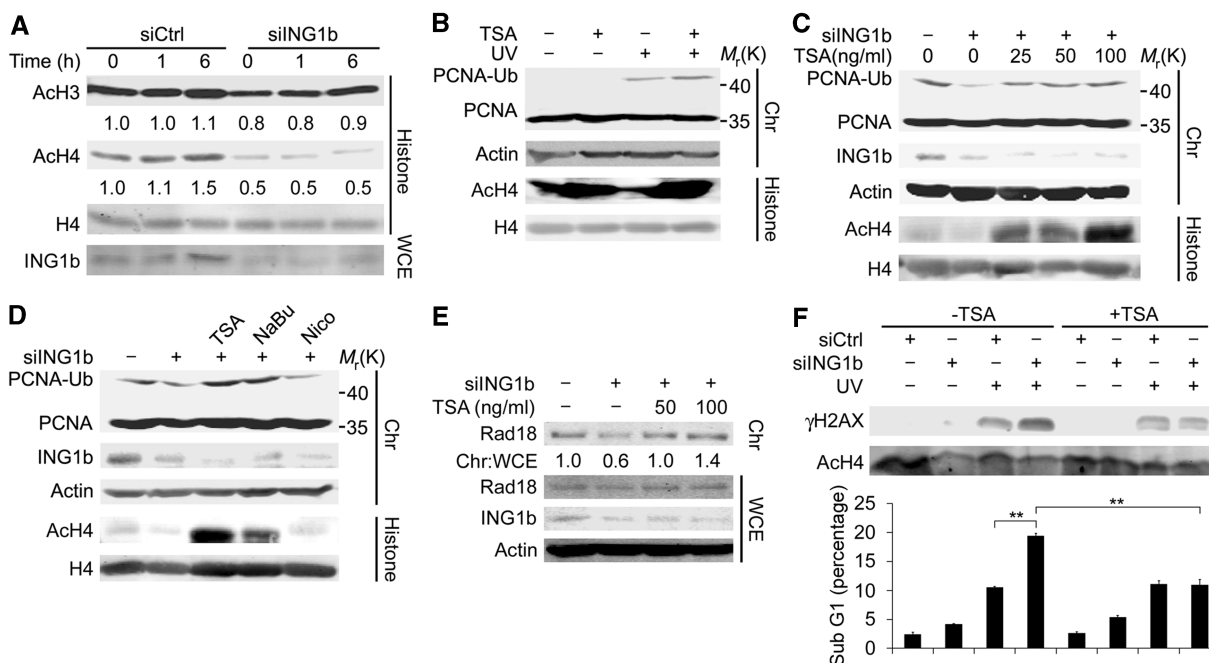


Figure 5. ING1b maintains histone H4 acetylation during S phase and is required for Rad18-mediated PCNA-Ub. (A) ING1b maintains AcH4 at S phase. Control and ING1b KD HCT116 cells were synchronized at G1-S boundary as in Figure 2B and irradiated with 10J/m^2 UVC. (B) TSA treatment enhances PCNA-Ub after UV. HCT116 cells pretreated with 50 ng/ml TSA for 1 h were irradiated with 10J/m^2 UVC and incubated with TSA for 6 h. (C) TSA treatment restores PCNA-Ub in ING1b KD cells. Control and ING1b KD HCT116 cells were treated with various doses of TSA and irradiated with 10J/m^2 UVC for 6 h. (D) TSA and sodium butyrate (NaBu) but not nicotinamide (Nico) restores PCNA-Ub in ING1b KD cells. Control and ING1b KD HCT116 cells were treated with 50 ng/ml TSA, 2.5 mM NaBu or 5 mM Nico and irradiated with 10J/m^2 UVC for 6 h. (E) TSA treatment restores Rad18 binding to chromatin after UV. Control and ING1b KD HCT116 cells were treated with various doses of TSA for 1 h and irradiated with 10J/m^2 UVC for 6 h. WCE and chromatin fraction were isolated for WB. Relative binding of Rad18 to chromatin is calculated as Chr:WCE. (F) TSA treatment alleviates genomic instability in ING1b depleted cells. HCT116 control and ING1b KD cells were treated with or without 5 ng/ml TSA, irradiated with 10J/m^2 UVC for 24 h. Cells were harvested for WB and FACS analysis. Data were presented as mean \pm SEM from three independent experiments (** $P < 0.01$).

in ING1b KD cells (Figure 5C), indicating that histone hyperacetylation bypasses the requirement of ING1b in PCNA-Ub. Moreover, we found that treatment of TSA and NaBu, HDAC class I and II inhibitors, but not treatment with nicotinamide, a NAD-dependent HDAC inhibitor, restored PCNA-Ub in ING1b KD cells (Figure 5D). We asked if ING1b regulates Rad18 through histone acetylation. Rad18 binding to chromatin was reduced in ING1b KD cells (Figures 4A and 5E). TSA treatment at various doses restored Rad18 binding to chromatin while the overall Rad18 expression did not change significantly (Figure 5E). We determined whether restoration of AcH4 in ING1b KD cells would rescue genomic instability and cell survival. Since TSA treatment was shown to induce apoptosis in HCT116 cells upon prolonged treatment (36,37), we performed the experiment at a reduced dose of TSA (5 ng/ml) which did not cause significant apoptosis, while AcH4 was restored in ING1b KD cells at this dose (Figure 5F). We observed that restoration of AcH4 by TSA alleviated UV-induced γH2AX and UV-induced apoptosis in ING1b KD cells (Figure 5F). This suggests that ING1b regulates PCNA-Ub and genomic stability through maintaining H4 acetylation during S phase. These data suggest that ING1b is required for stabilization of the stalled replication fork through maintenance of histone H4 acetylation

to mediate PCNA-Ub and lesion bypass, maintaining genomic stability (Figure 6).

DISCUSSION

In this study, we characterized the physiological role of ING1b in the UV response. Although it was previously shown that ING1b-deficient cells were more sensitive to UV irradiation (25,26), the mechanism by which ING1b status affects UV sensitivity is unknown. Consistent with previous findings, we observed that ING1b depleted cells were more sensitive to UV irradiation (Figure 1B). ING1b KD cells showed defects in recovering from UV-induced stalled replication and eventually became apoptotic (Figure 1C and D). Furthermore, we observed that replication fork progression was inhibited in ING1b KD cells after UVR (Figure 2B). As a result, there was an increased formation of DSBs and elevated chromosomal aberrations in ING1b KD cells (Figure 2C-E). We conclude that ING1b is required for overcoming blocked replication forks due to the presence of UV lesions during DNA replication. Therefore, in the absence of ING1b, stalled replication remains unresolved and prolonged replication blockage leads to catastrophic events such as chromatid breaks and chromosomal fusions.

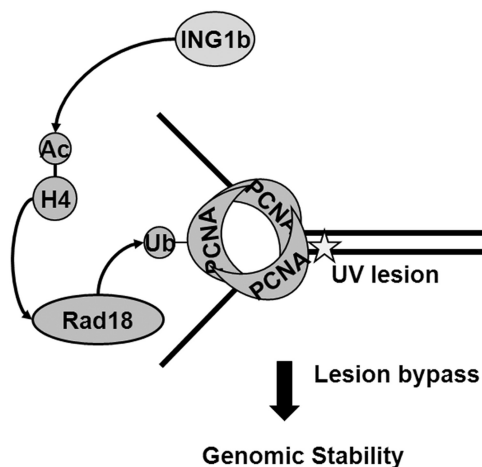


Figure 6. Model of ING1b in regulating histone H4 acetylation and Rad18-mediated PCNA-Ub upon replication stalling to facilitate lesion bypass and maintenance of genomic stability.

It has also been shown that ING1b overexpression increases stress-induced apoptosis including UV in a p53-dependent manner (38,39). We reasoned that ING1b may play a separate role in apoptosis and S phase recovery. At 10J/m^2 UVC, cells were allowed to progress throughout the cell cycle (Figure 1C) and therefore mechanisms involved in resolving stalled replication due to UV lesions would be essential for cell survival. In fact, we found that ING1b is required for monoubiquitination of PCNA which is central in regulating the lesion bypass mechanism to recover from stalled replication (5,6). Replication could be stalled even by the presence of very low levels of DNA lesions. We observed that PCNA-Ub and AcH4 are reduced in ING1b KD cells irradiated with a sub-lethal dose of UV (1J/m^2) (Supplementary Figure S10) suggesting a specialized role of ING1b in S phase recovery. In fact, our observation in ING1b KD cells is comparable with cells deficient in Rad18 E3 ligase, which is essential for PCNA-Ub. Rad18-deficient cells were found to be hypersensitive to DNA damaging agents and displayed enhanced genomic instability (40,41). Although we found that ING1b is required for Rad18-dependent PCNA-Ub, we also observed that co-KD of ING1b and Rad18 further reduced PCNA-Ub and sensitized cells to UV compared to ING1b and Rad18 KD alone (Supplementary Figure S12). This can be explained by the fact that Rad18 is not the only E3 ligase known to monoubiquitinate PCNA. Recently, another E3 ligase, CRL4(Cdt2), was found to monoubiquitinate PCNA in a Rad18-independent manner (42). Moreover, PCNA-Ub was found to be negatively regulated by the deubiquitinating enzyme, ubiquitin specific protease 1 (USP1) which removes ubiquitin from PCNA (43). ING1b might regulate PCNA-Ub and cell survival upon replication stress through these molecules. We observed that ING1b is required for the translesion DNA polymerase, Pol η , to form foci which are required for TLS (9,44) and for the interaction of Pol η specifically with the

monoubiquitinated form of PCNA. The ability of Pol η to interact with PCNA through the Ub-binding zinc finger (UBZ) and the newly identified PCNA interacting domains are all required for full activation of TLS (45). We postulate that ING1b is required for efficient PCNA-Ub in initiating TLS to bypass the UV lesions at stalled forks.

We further demonstrated that ING1b is required for histone H4 acetylation at S phase (Figure 5A) and that TSA treatment which induces histone hyperacetylation enhances PCNA-Ub (Figure 5B). During replication, new histone H4 is acetylated at K5 and K12 prior to assembly into chromatin and deacetylation occurs within 30–60 min. Inhibition of deacetylation may preserve AcH4 after chromatin assembly. This may explain why treatment with HDAC inhibitors bypasses the requirement of ING1b in PCNA-Ub (Figure 5C and D). Our results also indicate that reduction of AcH4 in ING1b KD cells during non-stress conditions does not lead to a significant retardation in normal S phase progression (Supplementary Figure S4), suggesting that reduction of AcH4 is not due to inhibition of DNA replication. Our observation, in part, corresponds with work previously done in yeast. Choy and Kron observed that cells deficient in Yng2, the yeast homologue of ING proteins, are highly sensitive to replication stress, including UV, hydroxyurea and MMS. Moreover, *yng2* mutants showed a reduction in histone H4 acetylation and delayed S phase progression upon MMS treatment. In addition, TSA treatment alleviates the S phase delay in *yng2* mutants after MMS treatment (46) which concurs with our observation that restoration of AcH4 in ING1b depleted cells rescues UV-induced DNA DSBs and apoptosis (Figure 5F). It indicates that the regulation of histone H4 acetylation and recovery from replication stress is conserved in eukaryotes. Other members of ING family proteins have also been implicated in regulating DNA replication to preserve genomic stability (47). The ING5 complex containing HBO1 is required for normal DNA replication (20). Recently, ING2 was also shown to be required for normal DNA replication and is associated with PCNA (24). In the same study, the authors observed that ING1b is not involved in normal DNA replication which coincides with our observation (24). Our study suggests that ING1 plays a unique role in DNA replication upon stress.

Why is histone acetylation required for PCNA-Ub? Chromatin is a barrier for DNA replication and repair. It has to be remodelled before these processes are possible (48,49). We previously showed that ING1b regulates histone H4 acetylation and chromatin relaxation to provide accessibility for XPA in nucleotide excision repair (25). It is possible that ING1b remodels the chromatin structure through H4 acetylation to provide accessibility for factors involved in lesion bypass. This is supported by the observation that Rad18 and Pol η binding to chromatin was reduced in ING1b KD cells (Figure 4A) and TSA treatment restores Rad18 binding to chromatin in ING1b KD cells (Figure 5E). In fact, chromatin remodelling enzymes are found to be important for DNA replication upon stress. For instance, the

ATP-dependent chromatin remodelling enzyme Ino80 is found to associate directly with replication forks and is required for fork stability and restart upon stress (50,51). More recently, Ino80 was also found to be required for PCNA-Ub (52). Moreover, it has been shown that alterations in chromatin structure affect Pol η dynamics in TLS (53). ING1b depletion did not affect expression of the ATP-dependent chromatin remodelling factors BRG1 and SNF5 (Supplementary Figure S13) which suggests a more direct and distinct role of ING1b in regulation of lesion bypass. Therefore, it is conceivable that ING1b may affect replication fork stability in S phase recovery.

In conclusion, our data provide evidence for the physiological role of ING1b in the recovery from replication blockage through regulation of PCNA-Ub and histone H4 acetylation. To our knowledge, this is the first study linking histone acetylation to the PCNA-Ub pathway. Our study provides a novel insight into the regulation of lesion bypass mechanism and implicates the role of ING1b in genomic stability and tumour suppression.

SUPPLEMENTARY DATA

Supplementary Data are available at NAR Online.

ACKNOWLEDGEMENTS

We thank Dr A.R. Lehmann, Dr K. Myung, Dr J. Furukawa, Dr S. Jamil and Dr Y. Wang for reagents; Dr T. Lee and P. Wighton for technical support and Dr V. Duronio for reading the manuscript.

FUNDING

Canadian Institutes of Health Research (MOP-84559 and MOP-93810) and Canadian Dermatology Foundation (to G.L.). National Cancer Institute of Canada (to R.P.C.W., studentship). Natural Sciences and Engineering Research Council of Canada (to H.L. and S.K., scholarship). Canadian Institutes of Health Research Skin Research Training Centre (to R.P.C.W., H.L. and B.P., scholarship). Funding for open access charge: Canadian Institutes of Health Research.

Conflict of interest statement. None declared.

REFERENCES

- Kunkel, T.A. (2004) DNA replication fidelity. *J. Biol. Chem.*, **279**, 16895–16898.
- van Gent, D.C., Hoeijmakers, J.H. and Kanaar, R. (2001) Chromosomal stability and the DNA double-stranded break connection. *Nat. Rev. Genet.*, **2**, 196–206.
- Lehmann, A.R. (2006) Translesion synthesis in mammalian cells. *Exp. Cell Res.*, **312**, 2673–2676.
- Chiu, R.K., Brun, J., Ramaekers, C., Theys, J., Weng, L., Lambin, P., Gray, D.A. and Wouters, B.G. (2006) Lysine 63-polyubiquitination guards against translesion synthesis-induced mutations. *PLoS Genet.*, **2**, e116.
- Hoegge, C., Pfander, B., Moldovan, G.L., Pyrowolakis, G. and Jentsch, S. (2002) RAD6-dependent DNA repair is linked to modification of PCNA by ubiquitin and SUMO. *Nature*, **419**, 135–141.
- Stelter, P. and Ulrich, H.D. (2003) Control of spontaneous and damage-induced mutagenesis by SUMO and ubiquitin conjugation. *Nature*, **425**, 188–191.
- Ulrich, H.D. (2005) The RAD6 pathway: control of DNA damage bypass and mutagenesis by ubiquitin and SUMO. *ChemBiochem*, **6**, 1735–1743.
- Watanabe, K., Tateishi, S., Kawasuji, M., Tsurimoto, T., Inoue, H. and Yamaizumi, M. (2004) Rad18 guides poleta to replication stalling sites through physical interaction and PCNA monoubiquitination. *Embo J.*, **23**, 3886–3896.
- Kannouche, P.L., Wing, J. and Lehmann, A.R. (2004) Interaction of human DNA polymerase η with monoubiquitinated PCNA: a possible mechanism for the polymerase switch in response to DNA damage. *Mol. Cell*, **14**, 491–500.
- Niimi, A., Brown, S., Sabbioneda, S., Kannouche, P.L., Scott, A., Yasui, A., Green, C.M. and Lehmann, A.R. (2008) Regulation of proliferating cell nuclear antigen ubiquitination in mammalian cells. *Proc. Natl Acad. Sci. USA*, **105**, 16125–16130.
- Lehmann, A.R., Niimi, A., Ogi, T., Brown, S., Sabbioneda, S., Wing, J.F., Kannouche, P.L. and Green, C.M. (2007) Translesion synthesis: Y-family polymerases and the polymerase switch. *DNA Repair*, **6**, 891–899.
- Ling, H., Boudsocq, F., Plosky, B.S., Woodgate, R. and Yang, W. (2003) Replication of a cis-syn thymine dimer at atomic resolution. *Nature*, **424**, 1083–1087.
- Trincao, J., Johnson, R.E., Escalante, C.R., Prakash, S., Prakash, L. and Aggarwal, A.K. (2001) Structure of the catalytic core of *S. cerevisiae* DNA polymerase η : implications for translesion DNA synthesis. *Mol. Cell*, **8**, 417–426.
- Acharya, N., Yoon, J.H., Gali, H., Unk, I., Haraeska, L., Johnson, R.E., Hurwitz, J., Prakash, L. and Prakash, S. (2008) Roles of PCNA-binding and ubiquitin-binding domains in human DNA polymerase η in translesion DNA synthesis. *Proc. Natl Acad. Sci. USA*, **105**, 17724–17729.
- Limoli, C.L., Giedzinski, E., Bonner, W.M. and Cleaver, J.E. (2002) UV-induced replication arrest in the xeroderma pigmentosum variant leads to DNA double-strand breaks, gamma-H2AX formation, and Mre11 relocalization. *Proc. Natl Acad. Sci. USA*, **99**, 233–238.
- Wang, Y., Woodgate, R., McManus, T.P., Mead, S., McCormick, J.J. and Maher, V.M. (2007) Evidence that in xeroderma pigmentosum variant cells, which lack DNA polymerase η , DNA polymerase ι causes the very high frequency and unique spectrum of UV-induced mutations. *Cancer Res.*, **67**, 3018–3026.
- Moriwaki, S. and Kraemer, K.H. (2001) Xeroderma pigmentosum—bridging a gap between clinic and laboratory. *Photodermatol. Photoimmunol. Photomed.*, **17**, 47–54.
- Shi, X., Hong, T., Walter, K.L., Ewalt, M., Michishita, E., Hung, T., Carney, D., Pena, P., Lan, F., Kaadige, M.R. *et al.* (2006) ING2 PHD domain links histone H3 lysine 4 methylation to active gene repression. *Nature*, **442**, 96–99.
- Pena, P.V., Davrazou, F., Shi, X., Walter, K.L., Verkhusha, V.V., Gozani, O., Zhao, R. and Kutateladze, T.G. (2006) Molecular mechanism of histone H3K4me3 recognition by plant homeodomain of ING2. *Nature*, **442**, 100–103.
- Doyon, Y., Cayrou, C., Ullah, M., Landry, A.J., Cote, V., Selleck, W., Lane, W.S., Tan, S., Yang, X.J. and Cote, J. (2006) ING tumor suppressor proteins are critical regulators of chromatin acetylation required for genome expression and perpetuation. *Mol. Cell*, **21**, 51–64.
- Doyon, Y., Selleck, W., Lane, W.S., Tan, S. and Cote, J. (2004) Structural and functional conservation of the NuA4 histone acetyltransferase complex from yeast to humans. *Mol. Cell Biol.*, **24**, 1884–1896.
- Vieyra, D., Loewith, R., Scott, M., Bonnefin, P., Boisvert, F.M., Cheema, P., Pastyryeva, S., Meijer, M., Johnston, R.N., Bazett-Jones, D.P. *et al.* (2002) Human ING1 proteins differentially regulate histone acetylation. *J. Biol. Chem.*, **277**, 29832–29839.
- Skowyra, D., Zeremski, M., Neznanov, N., Li, M., Choi, Y., Uesugi, M., Hauser, C.A., Gu, W., Gudkov, A.V. and Qin, J. (2001) Differential association of products of alternative transcripts of the candidate tumor suppressor ING1 with the mSin3/HDAC1

- transcriptional corepressor complex. *J. Biol. Chem.*, **276**, 8734–8739.
24. Larrieu, D., Ythier, D., Binet, R., Brambilla, C., Brambilla, E., Sengupta, S. and Pedoux, R. (2009) ING2 controls the progression of DNA replication forks to maintain genome stability. *EMBO Rep.*, **10**, 1168–1174.
 25. Kuo, W.H., Wang, Y., Wong, R.P., Campos, E.I. and Li, G. (2007) The ING1b tumor suppressor facilitates nucleotide excision repair by promoting chromatin accessibility to XPA. *Exp. Cell Res.*, **313**, 1628–1638.
 26. Kichina, J.V., Zeremski, M., Aris, L., Gurova, K.V., Walker, E., Franks, R., Nikitin, A.Y., Kiyokawa, H. and Gudkov, A.V. (2006) Targeted disruption of the mouse *ing1* locus results in reduced body size, hypersensitivity to radiation and elevated incidence of lymphomas. *Oncogene*, **25**, 857–866.
 27. Li, G., Tang, L., Zhou, X., Tron, V. and Ho, V. (1998) Chemotherapy-induced apoptosis in melanoma cells is p53 dependent. *Melanoma Res.*, **8**, 17–23.
 28. Lengauer, C., Kinzler, K.W. and Vogelstein, B. (1997) Genetic instability in colorectal cancers. *Nature*, **386**, 623–627.
 29. Cahill, D.P., Lengauer, C., Yu, J., Riggins, G.J., Willson, J.K., Markowitz, S.D., Kinzler, K.W. and Vogelstein, B. (1998) Mutations of mitotic checkpoint genes in human cancers. *Nature*, **392**, 300–303.
 30. Li, J., Wang, Y., Wong, R.P. and Li, G. (2009) The role of ING tumor suppressors in UV stress response and melanoma progression. *Curr. Drug Targets*, **10**, 455–464.
 31. Aguiusa-Toure, A.H., Wong, R.P. and Li, G. (2011) The ING family tumor suppressors: from structure to function. *Cell Mol. Life Sci.*, **68**, 45–54.
 32. Garate, M., Campos, E.I., Bush, J.A., Xiao, H. and Li, G. (2007) Phosphorylation of the tumor suppressor p33(ING1b) at Ser-126 influences its protein stability and proliferation of melanoma cells. *FASEB J.*, **21**, 3705–3716.
 33. Coles, A.H., Liang, H., Zhu, Z., Marfella, C.G., Kang, J., Imbalzano, A.N. and Jones, S.N. (2007) Deletion of p37Ing1 in mice reveals a p53-independent role for Ing1 in the suppression of cell proliferation, apoptosis, and tumorigenesis. *Cancer Res.*, **67**, 2054–2061.
 34. Giacca, M., Zentilin, L., Norio, P., Diviacco, S., Dimitrova, D., Contreas, G., Biamonti, G., Perini, G., Weighardt, F., Riva, S. *et al.* (1994) Fine mapping of a replication origin of human DNA. *Proc. Natl Acad. Sci. USA*, **91**, 7119–7123.
 35. Davies, A.A., Huttner, D., Daigaku, Y., Chen, S. and Ulrich, H.D. (2008) Activation of ubiquitin-dependent DNA damage bypass is mediated by replication protein a. *Mol. Cell*, **29**, 625–636.
 36. Mattera, L., Escaffit, F., Pillaire, M.J., Selves, J., Tyteca, S., Hoffmann, J.S., Gourraud, P.A., Chevillard-Briet, M., Cazaux, C. and Trouche, D. (2009) The p400/Tip60 ratio is critical for colorectal cancer cell proliferation through DNA damage response pathways. *Oncogene*, **28**, 1506–1517.
 37. Sayan, B.S., Sayan, A.E., Yang, A.L., Aqeilan, R.I., Candi, E., Cohen, G.M., Knight, R.A., Croce, C.M. and Melino, G. (2007) Cleavage of the transactivation-inhibitory domain of p63 by caspases enhances apoptosis. *Proc. Natl Acad. Sci. USA*, **104**, 10871–10876.
 38. Cheung, K.J. Jr. and Li, G. (2002) p33(ING1) enhances UVB-induced apoptosis in melanoma cells. *Exp. Cell Res.*, **279**, 291–298.
 39. Garkavtsev, I., Grigorian, I.A., Ossovskaya, V.S., Chernov, M.V., Chumakov, P.M. and Gudkov, A.V. (1998) The candidate tumour suppressor p33ING1 cooperates with p53 in cell growth control. *Nature*, **391**, 295–298.
 40. Tateishi, S., Sakuraba, Y., Masuyama, S., Inoue, H. and Yamaizumi, M. (2000) Dysfunction of human Rad18 results in defective postreplication repair and hypersensitivity to multiple mutagens. *Proc. Natl Acad. Sci. USA*, **97**, 7927–7932.
 41. Tateishi, S., Niwa, H., Miyazaki, J., Fujimoto, S., Inoue, H. and Yamaizumi, M. (2003) Enhanced genomic instability and defective postreplication repair in RAD18 knockout mouse embryonic stem cells. *Mol. Cell. Biol.*, **23**, 474–481.
 42. Terai, K., Abbas, T., Jazaeri, A.A. and Dutta, A. (2010) CRL4(Cdt2) E3 ubiquitin ligase monoubiquitinates PCNA to promote translesion DNA synthesis. *Mol. Cell*, **37**, 143–149.
 43. Huang, T.T., Nijman, S.M., Mirchandani, K.D., Galardy, P.J., Cohn, M.A., Haas, W., Gygi, S.P., Ploegh, H.L., Bernards, R. and D'Andrea, A.D. (2006) Regulation of monoubiquitinated PCNA by DUB autocleavage. *Nat. Cell Biol.*, **8**, 339–347.
 44. Garg, P. and Burgers, P.M. (2005) Ubiquitinated proliferating cell nuclear antigen activates translesion DNA polymerases eta and REV1. *Proc. Natl Acad. Sci. USA*, **102**, 18361–18366.
 45. Bienko, M., Green, C.M., Sabbioneda, S., Crosetto, N., Matic, I., Hibbert, R.G., Begovic, T., Niimi, A., Mann, M., Lehmann, A.R. *et al.* (2010) Regulation of translesion synthesis DNA polymerase eta by monoubiquitination. *Mol. Cell*, **37**, 396–407.
 46. Choy, J.S. and Kron, S.J. (2002) NuA4 subunit Yng2 function in intra-S-phase DNA damage response. *Mol. Cell. Biol.*, **22**, 8215–8225.
 47. Larrieu, D. and Pedoux, R. (2009) SharING out the roles in replicating DNA. *Cell Cycle*, **8**, 3623–3624.
 48. Groth, A., Rocha, W., Verreault, A. and Almouzni, G. (2007) Chromatin challenges during DNA replication and repair. *Cell*, **128**, 721–733.
 49. Peterson, C.L. and Cote, J. (2004) Cellular machineries for chromosomal DNA repair. *Genes Dev.*, **18**, 602–616.
 50. Papamichos-Chronakis, M. and Peterson, C.L. (2008) The Ino80 chromatin-remodeling enzyme regulates replisome function and stability. *Nat. Struct. Mol. Biol.*, **15**, 338–345.
 51. Shimada, K., Oma, Y., Schleker, T., Kugou, K., Ohta, K., Harata, M. and Gasser, S.M. (2008) Ino80 chromatin remodeling complex promotes recovery of stalled replication forks. *Curr. Biol.*, **18**, 566–575.
 52. Falbo, K.B., Alabert, C., Katou, Y., Wu, S., Han, J., Wehr, T., Xiao, J., He, X., Zhang, Z., Shi, Y. *et al.* (2009) Involvement of a chromatin remodeling complex in damage tolerance during DNA replication. *Nat. Struct. Mol. Biol.*, **16**, 1167–1172.
 53. Sabbioneda, S., Gourdin, A.M., Green, C.M., Zotter, A., Giglia-Mari, G., Houtsmuller, A., Vermeulen, W. and Lehmann, A.R. (2008) Effect of proliferating cell nuclear antigen ubiquitination and chromatin structure on the dynamic properties of the Y-family DNA polymerases. *Mol. Biol. Cell*, **19**, 5193–5202.